

# Viscoelastic Influence on the Board Level Assessment of Wafer Level Packages Under Drop Impact and Under Thermal Cycling

Abel Misrak, Rabin Bhandari, Dereje Agonafer

The University of Texas at Arlington, Arlington, TX

Abstract

Structural components such as printed circuit boards (PCBs) are critical in the th assessment of electronic packages. Previous studies have shown that geometric mameters such as thickness and mechanical properties like elastic modulus of PCBs have direct influence on the reliability of electronic packages. Elastic material properties of PCBs are commonly characterized thing equipment such as tensile testers and used in computational studies. However, in certain application scoelastic material properties are important. Viscoelastic influence on materials is evident when one exceeds the glass transition temperature of materials. Operating conditions or manufacturing conditions such as lamination and soldering may expose components to temperatures that exceed the glass transition temperatures. Knowing the viscoelastic behavior of the different components of electronic backages is important in order to perform accurate reliability assessment and design components such a printed circuit boards (PCBs) that will remain dimensionally stable after the manufacturing process. Revious researchers have used creep and stress relaxation test data to obtain the Prony series terms the epresent the viscoelastic behavior and perform analysis. Others have used dynamic mechanical analysis in order to obtain frequency domain master curves that were converted to time domain before obtaining in Prony series terms. In this paper, nonlinear solvers were used on frequency domain master curve regular from dynamic mechanical analysis to obtain Prony on the impact of adding viscoelastic properties when series terms and perform finite element analy performing reliability assessment. The comparational study results were used to perform comparative assessment to understand the impact of including viscoelastic behavior in reliability analysis under thermal Cop Scale Packages. cycling and drop testing for Wafer Leve

Keywords: storage modulus, loss mod tus, shift functions, glass transition temperature, Prony series



#### I. INTRODUCTION

Ensuring the reliability of products is one of the main targets in the design of electronic systems. Reliability is defined as "the statistical probability that a device or system will operate without failure for a specified period" [1]. Reliability of electronic systems is impacted by various environmental loads including thermal and mechanical loads. From earlier studies conducted by US navy, the failure rate of electronic equipment was observed to have increased by eight-fold when deliberately exposed to temperature of more than 20 °C [2]. Increasing the operating temperature also have a negative impact on reliability. According to Yeh et. al., a 2°C increase in operating temperature reduces the reliability of silicon chappy 10 % [1]. For these reasons, there is a focus on performing extensive reliability studies before adupment are shipped to customers.

The reliability of products is often described with the use of "bathtub" die wim. High infant mortalities are observed due to bad product quality. Burn-in and run-in tests are often employed to catch early failures before products are shipped out. Failure rates due to wear out are reduced though improved designs, and guidelines such as IPC-D-279 (Design guidelines for Reliable Surface Mount Technology Printed Board Assemblies) are established to help designers [3]. Depending on the application electronic components will be exposed to mechanical shock, mechanical vibration, temperature cycling, or high humidity environments. The reliability of electronic assembly is determined by use conditions, the design life, and acceptable failure probability rates [3]. For example, a failure risk of < 0.1 km may be acceptable for computers, but a failure risk of < 0.001% is needed for commercial aircraft applications [4].

Thermal cycling and drop testing are two of the most common environmental loading conditions used to assess reliability of electronic equipment such as cell phones. Consumer products such as cell phones and cameras are susceptible to be dropped due to their size and weight [5]. The input acceleration from dropping results in mechanical failure on components such as housing and electrical failures due to cracking of printed circuit boards (PCBs) and solder interconnections [5]. On the other hand, the temperature swing experienced by various electronic products may range from 60 °C for consumer products, to more than 140 °C for electronics in automotive used under the hood of cars [4]. The temperature swings combined with the mismatch of CTE of the different materials used for packaging, subject critical components such as solder joints to stress and strain, eventuall chading to failure [6].

In addition to providing electronic connections, solder joints are usually the sole mechanical attachment of electronic components to P(B) [3]. As such, one of the major reliability concerns in microelectronic packaging is the integrity of solder interconnections [7]. Solders are inhomogeneous structures, and their grain structure is inherer by unstable. Micro-voids start forming at the grain boundary ~25 % of the fatigue life, eventually coalesting to macro-cracks and leading to total fractures causing electrical failures [3]. Experimental tests of humarical techniques are used to study the thermo-mechanical reliability of solders and other components.

Experimental tests are often expensive and time consuming. To save cost, advanced finite element analysis is often performed during the design and development phases to ensure reliability of products [7]. Finite element analysis is also performed to predict field use limits and analyze field failures [6]. Using numerical techniques requires the use of life prediction methodologies that are based on the different damage

mechanisms observed in the field [7]. Numerous solder joint fatigue life prediction models such as Yamada [8], Engelmaier [9], Syed [10], Darveaux [11], can be found in the literature [7]. These different approaches can be grouped into four main categories: strain-based approach, energy-based approach, fracture mechanics-based approach, and evolution-based approach [12]. Darveaux's energy-based fatigue life prediction model has been widely used in the literature to predict the life of Pb-Sn solders [6]. Widely used fatigue life prediction model for lead free solders was proposed by Schubert et. al. and is used in this paper [13].

Different factors affect the accuracy of numerical studies. Capturing the correct boundary and load conditions, employing the correct numerical models, and obtaining accurate material properties for the components are some of the key challenges in obtaining accurate numerical results. Components such as solder are extremely inhomogeneous, and accurately capturing their material properties is challenging. The Anand viscoplastic constitutive model, originally proposed to study hot working of retals [14] [15], is widely used to model solders for computational studies [16]. The Anand model uses stress equation, flow equation, and evolution equation, and unifies the creep and rate-independent plastic behaviors of solder [16]. The nine material constants used to define the constitutive equations are experimentally characterized and used in computational studies [17]. Stress-Strain or Creep data measurements have been used in the literature to determine the Anand constants [16]. In this paper, Anand constants for SAC solders were obtained from [18] and used for computational studies.

nonic packages are modeled as elastic For structural simulations, most of the components in the el materials. For materials that go close to glass transition temperate. (Tg), viscoelastic material properties are often used to accurately capture the material behavior. Visco astic materials are materials that exhibit both viscous and elastic behaviors. The Maxwell model, initially proposed in 1867, captures the elastic and viscous properties using Newtonian damper and Hookia S ring [19]. However, the simple Maxwell model consisting of a single spring and damper in series law a limitation in modelling creep phenomenon. A generalized Maxwell model with multiple Maxwell branches in parallel as shown in Fig. 1 overcomes the limitations and is used to model viscoelastic margals. For the generalized model, time dependent shear moduli are represented using Prony series as shown in equations 1 below [19]. Taking the Laplace transform of equation 1 gives the *complex shear module* as shown in equation 2. The real part of the complex shear modulus is called storage shear modulus the complex part is called loss shear modulus [20]. Storage terms are shown in equations 3 - 4 [21]. The relative moduli  $(\alpha_i^G)$ and loss modulus in terms of Prony seri and relaxation time  $(\tau_i^G)$  terms can be entered to computational software such as ANSYS to capture the viscoelastic behavior of materials fromputational studies.

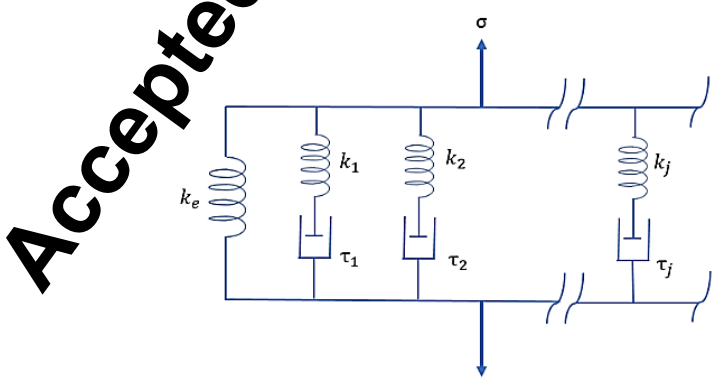


Fig. 1. General Maxwell model used to represent viscoelastic materials.

$$G(t) = G_0 \left[ \alpha_{\infty}^G + \sum_{i=1}^{n_G} \alpha_i^G \exp\left(-\frac{t}{\tau_i^G}\right) \right]$$
 (1)

$$G^*(j\omega) = G_{\infty} + \sum_{i=1}^{n_G} \frac{g_i^G \tau_i^G j\omega}{1 + \tau_i^G j\omega}$$
 (2)

$$G'(\omega) = R\{G^*\} = G_{\infty} + \sum_{i=1}^{n_G} g_i^G \frac{(\tau_i \omega)^2}{1 + (\tau_i \omega)^2}$$
(3)

$$G''(\omega) = I\{G^*\} = \sum_{i=1}^{n_G} g_i^G \frac{\tau_i^G \omega}{1 + (\tau_i^G \omega)^2}$$

#### Dynamic Mechanical Analysis

Dynamical mechanical analyzer (DMA) is a technique that applies oscill to g strain or stress and uses the result to measure the kinetic properties of samples [22]. The major components of DMA are shown in Fig. 2 below. Output of DMA consists of temperature dependent loss and torage moduli of materials at different frequencies. The relations between loss modulus, storage modulus, and complex modulus are given by equations 5 - 7 below. Using the "time-temperature superposition" the DMA results are expanded to a wider frequency range and a master curve is obtained. The detail of the procedures is discussed in the materials and methods section.

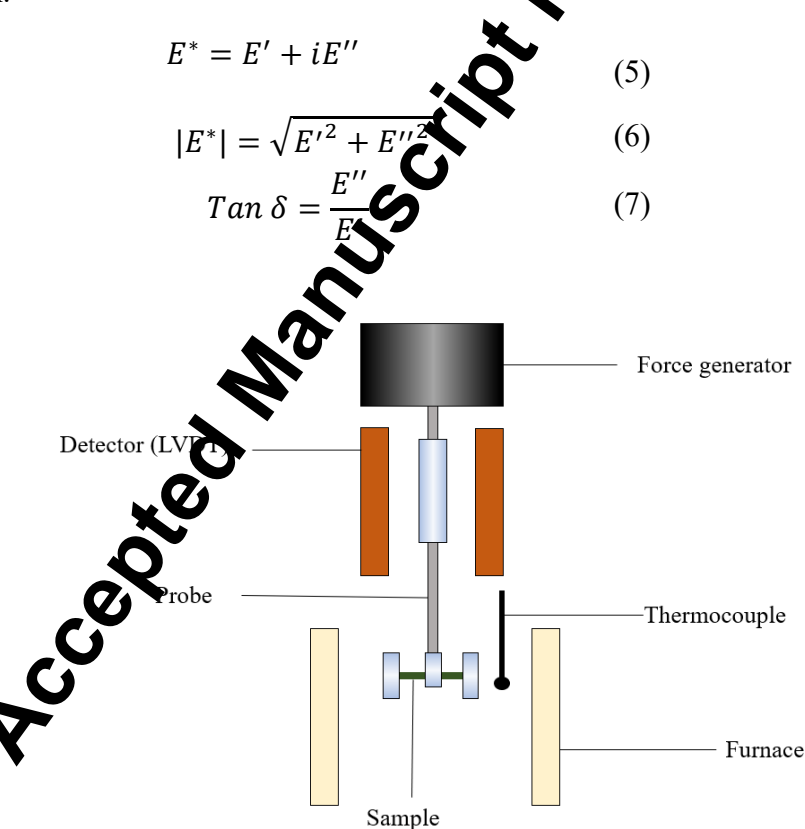


Fig. 2. Major components of DMA [22].

Shrotriya et. al. used creep data from DMA to develop a micromechanical model that can be used to understand the time-temperature dependent behavior of PCB substrates and understand residual stresses and dimensional changes in the PCBs during processing such as re-lamination and soldering processes [23]. On the other hand, Liu et. al. investigated the viscoelastic influence of PCBs evaluated under drop impact [24]. They showed that the viscoelasticity of PCBs has a distinct influence on the dynamic properties of PCBs under board-level impact, and proposed using PCB substrate with larger viscoelasticity and reduced size in order to improve drop impact reliability [24].

While running FEA simulations for reliability study of electronic packages, PCBs are represented using three different approaches: lumped board modeling approach, explicit geometry approach, and electronic computer aided design (ECAD) approach [25]. Lumped board approach represent PBs as blocks with effective mechanical properties. Explicit approach uses a layer-by-layer representation of PCBs, while ECAD approach uses the exact design files used to make PCBs. Explicit geometry ECAD approach give a more accurate representation of PCBs; however, lumped approach is componly used as the other approaches require very large mesh sizes and long solution times [25]. In lump approach, PCBs are characterized using only their orthotropic elastic material properties. However, for computational studies that involve drop impact, or for conditions where temperatures go near and beyond the glass transition temperature (T<sub>g</sub>), it is important to include the viscoelastic behavior in computational studies. In this paper, the frequency domain master curve obtained from dynamic mechanical analysis is used to obtain the Prony series terms which are used to model PCBs as viscoelastic material. Using the Static and Transient structural packages in ANSYS 2019 R1, the impact of including visco listic property of PCBs for board level reliability assessment of Wafer Level Packages (WLPs) is sudied. WLP is an advanced packaging technology where packages are fabricated and tested at the wafer level before singulation [26]. WLPs are used for applications such as analog devices, power mar ment devices, image sensors, and integrated passives [26]. In this paper, the reliability of WLPs is essessed under two different loading conditions: thermal cycling and drop impact. The details of the procedure for obtaining the Prony series terms are given in acction 2: the assurant in the latest terms are given in section 2; the computational model is discussed in section 3; results, discussion and conclusions are given in the subsequent sections.

### II. MATERIALS AND METHODS

Dynamic Mechanical Analyzer (DMC) has used to measure the frequency and temperature dependent storage (E') and loss (E'') moduli of Kan thick FR-4 based PCBs used for WLP. Measurements were run at frequencies of 0.5, 1, 5, 10, 20, 100 Hz. Fig. 3 below shows the equipment and sample attached for measurement using the dual cantile bending attachment, and cross section image of the PCB sample. Due to the thickness and the expected odulus of the sample, the tensile attachment of DMA was found to not be suitable for measurement. The reometric dimensions of the sample along with the test parameters used for DMA are given on Table 1, Fig. 4 shows a DMA result for the temperature and frequency dependent measurement of loss and storage modulus values.







Fig. 3. DMA7100 used for testing (left), samples attached using DMA anding mode (center), cross section of PCB sample (right).

TABEL I
GEOMETRIC DIMENSIONS OF SAMPLES AND TEST CARAMETERS USED FOR DMA
TESTING

	Parameters	Value
	Maximum Force	2000 mN
	Temperature Ra up	3 °C/min
	Sample Thicks:	1.01 mm
	Sample Lingth	20 mm
	Sam le Width	5.75 mm
A Cooker		

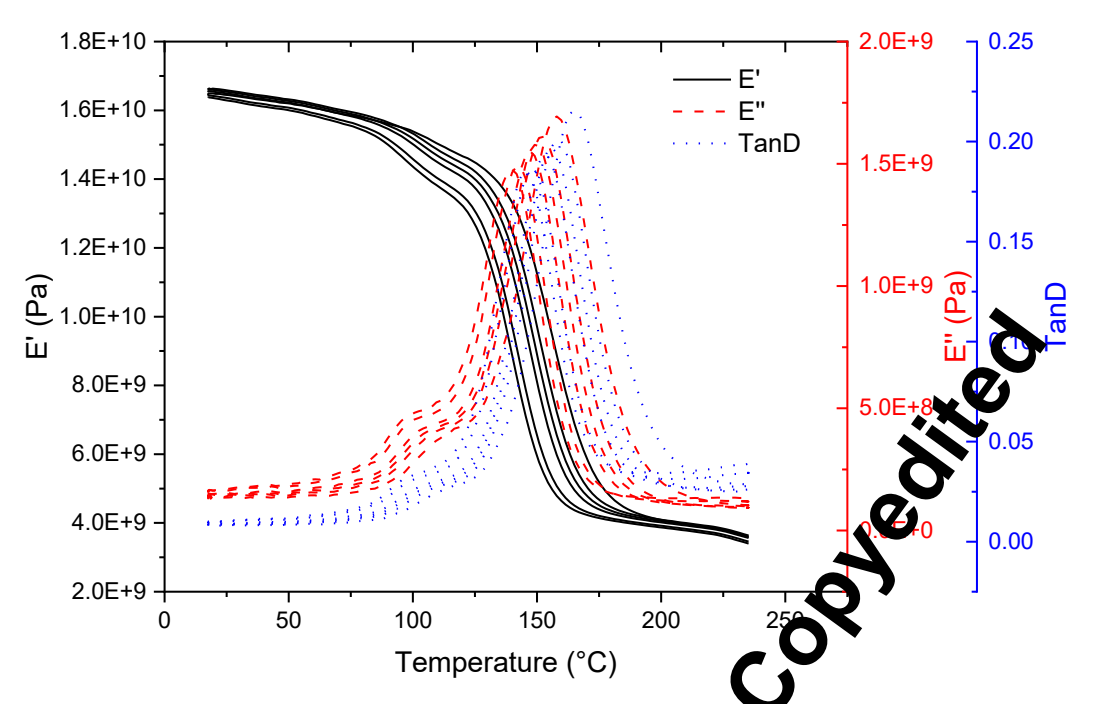


Fig. 4. DMA result showing temperature dependent storage modulus (black), loss modulus (red), and loss tangent (blue). Different lines correspond to a thrent frequencies.

After the DMA analysis, the built-in tool for DMA (TA 000) was used to generate the master curve showing the loss and storage moduli for a wider range of frequency values. An important input parameter in obtaining the master curve using shift functions is the glass ransition temperature ( $T_g$ ). Dynamic mechanical analysis is one of the widely used techniques to measure  $T_g$  [27]. Results for storage modulus (E'), loss modulus (E''), or  $Tan \delta$  from DMA measurements may be used to define the glass transition temperature. For results obtained for 1 Hz, the temperature values at the onset of E', peak of E'', or peak of  $Tan \delta$  can be considered the glass transition temperature [27]. The onset of E' is the most conservative of the three approaches and often relates to mechanical fancte [27]. In this paper, the onset of E' at 1 Hz is used to measure the  $T_g$  at 126.5 °C.

The master curve obtained from DM. reasurements is one of the available techniques for studying the frequency dependence of viscoelastic properties of materials [28]. The master curve is obtained by using the "time-temperature superposition" that exists in dynamic viscoelastic measurements. Initial measurements are performed at 6 frequencies and wide temperature range. However, by using the "time-temperature superposition", the viscoelastic properties are predicted for wider frequency ranges for a given temperature value [28]. This "time-temperature superposition" is achieved using the expanded William-Landel-Ferry (WLF) equation which is good by equation 8 below [28]. The corresponding master curve obtained showed loss and storage modulus as a function of frequency and is shown in Fig. 5 below. The WLF equation is best used to obtain the master curve for temperatures equal or greater than the glass transition temperature (Tg) [28]. For temperature adues lower than Tg, Arrehenius equation (given in equation 9) is preferred to describe the shift factor-temperature relationship and obtain master curves [29].

$$log \ a_T = \frac{c_1(T - T_g)}{c_2 + T - T_g} + \frac{c_1(T_r - T_g)}{c_2 + T_r - T_g}$$
 (8)

$$\ln a_T = \frac{E_a}{R} \left( \frac{1}{T} - \frac{1}{T_0} \right) \tag{9}$$

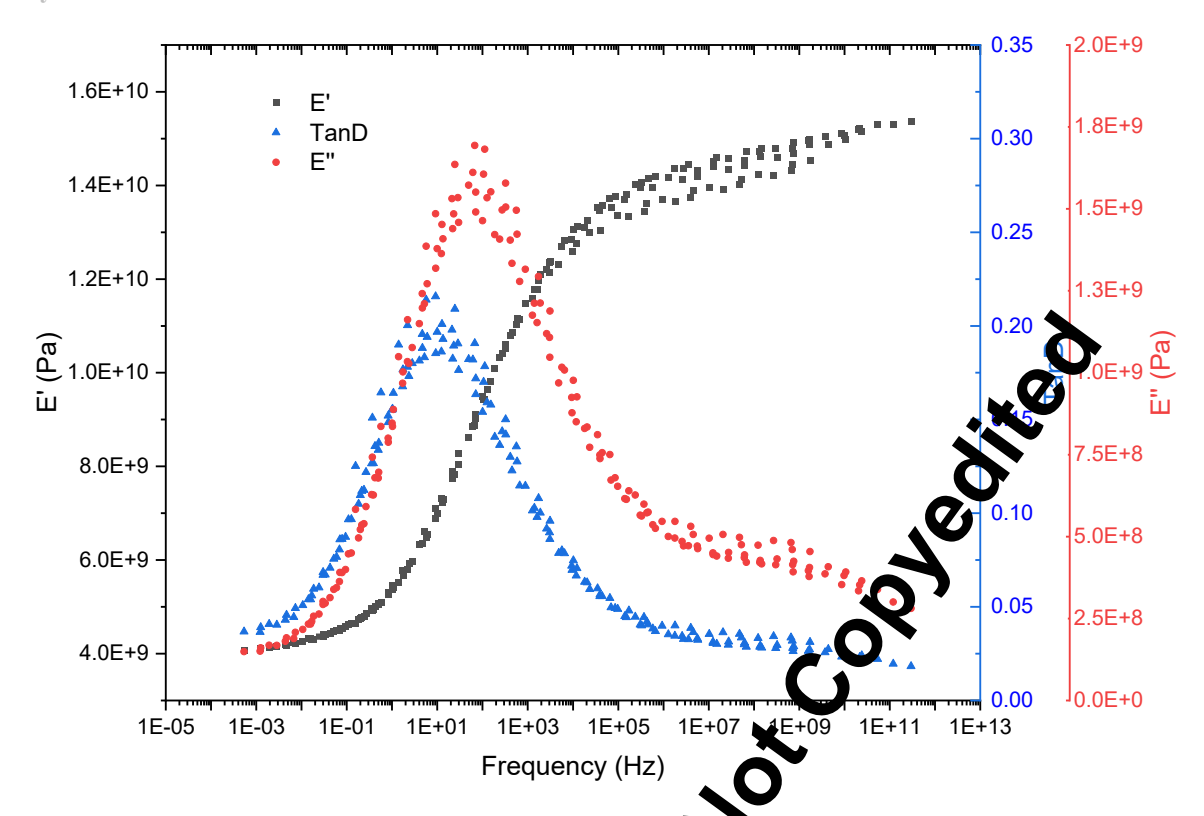


Fig. 5. Master curve showing storage modulus (black), loss modulus (red), and  $Tan \delta$  (blue) as a function of frequency.

Computational software such as ANSYS require visco to input Prony series coefficients to capture viscoelastic properties in simulations. The master curve shown in Fig. 5 is not in the form that can be included in simulations, and additional post processing is required to obtain the Prony series terms.

Obtaining the Prony series terms from master caves have been the focus of previous research, and different authors have used different approaches to obtain the time domain master curves and extract Prony series terms. Lakes [30] defined the interrelations between the moduli as:

$$\frac{2}{\pi}E''(\omega)|_{\omega} \approx -\frac{dE'(\omega)}{d\ln\omega} \approx -\frac{dE(t)}{d\ln t}$$
 (10)

With  $\tau = 1/t$ , equation 10 implies that:

$$E'(t) = \frac{1}{\tau} \approx E(t) \tag{11}$$

Previous studies on the or act of viscoelastic influence on PCBs [31] [32] [33] have made use of the relation given in equation (1) to shift the master curve to the time domain and extract the Prony series terms by performing nonlinear curve fitting. Other empirical equations, such as equation 12, have also been proposed to shift the squency domain master curve to time domain [34].

$$E(t) = E'(\omega) + 0.0004E'(0.02\omega) - 0.25E'(5\omega) + 0.35E'(0.2\omega)$$
 (12)

In this paper, the Prony series terms are obtained by performing nonlinear fit to the master curve in frequency domain using equations 3 and 4. Nonlinear parametric fitting tool on OriginPro was used to perform the curve fitting. "Wicket plot" was produced to determine the suitability of the measured data for the creation of master curve as shown in Fig. 6.

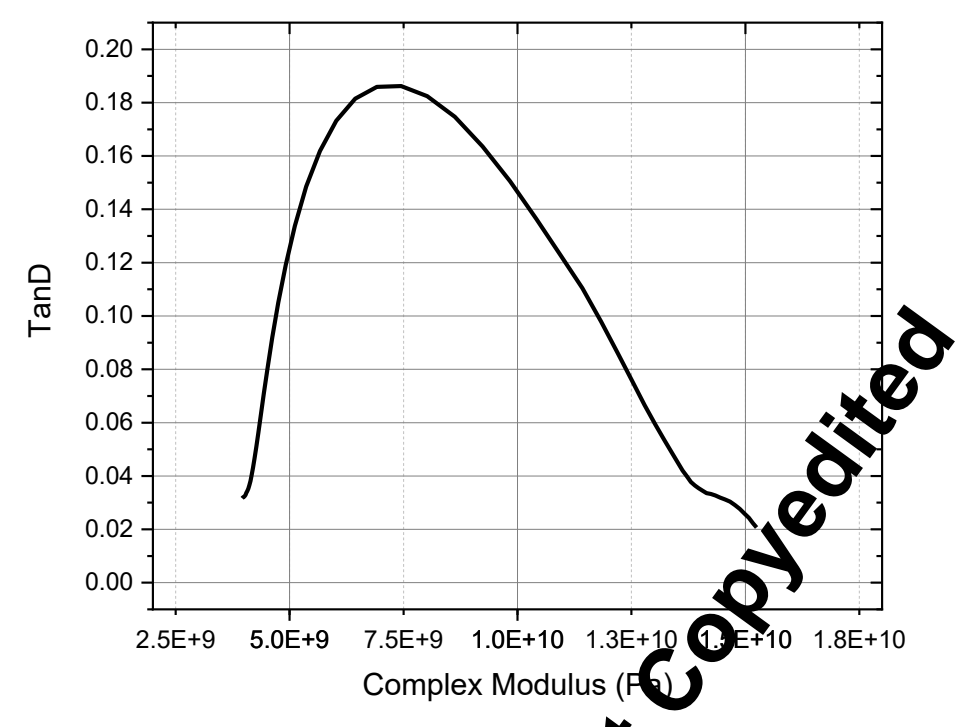


Fig. 6. Wicket Plot showing the relation between complex modulus and Tan  $\delta$ .

From the curve fitting,  $g_i^G$  and  $\tau_i^G$  were obtained. These terms were used in equation 1 to obtain  $G_0$ . Then the relative moduli terms were obtained using the relation  $\alpha_i^G = g_i^G/G_0$ . The fit parameters were tested by comparing the computed and measured complex modulus values. Comparison between computed and measured complex modulus values for 160 °C are shown in Fig. 7. Average difference between measured and fit values < 1%. A representative data for compared Prony series terms for 155 °C and 165 °C are given in Table II.

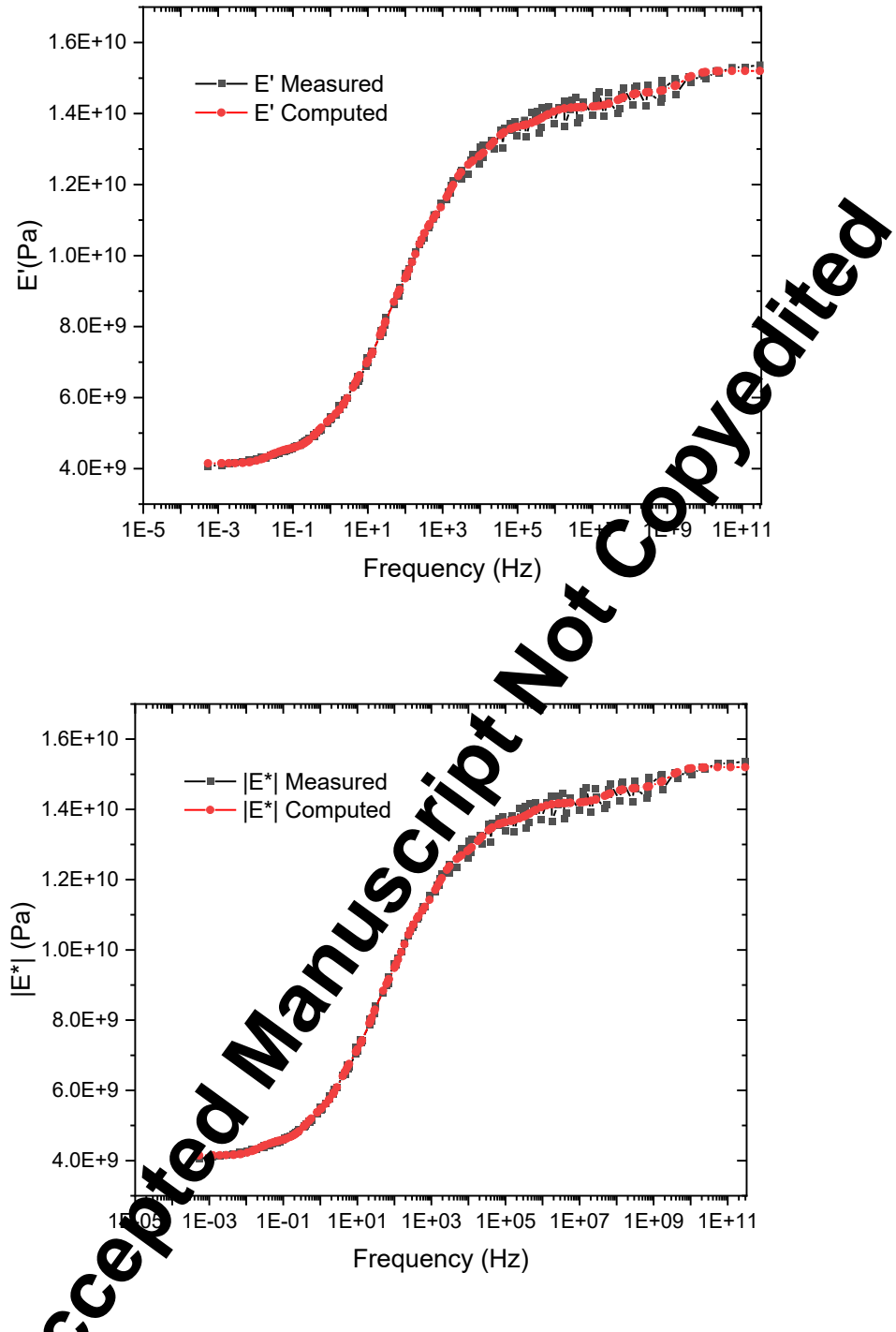


Fig. . Computed vs measured storage and complex modulus for 165 °C.

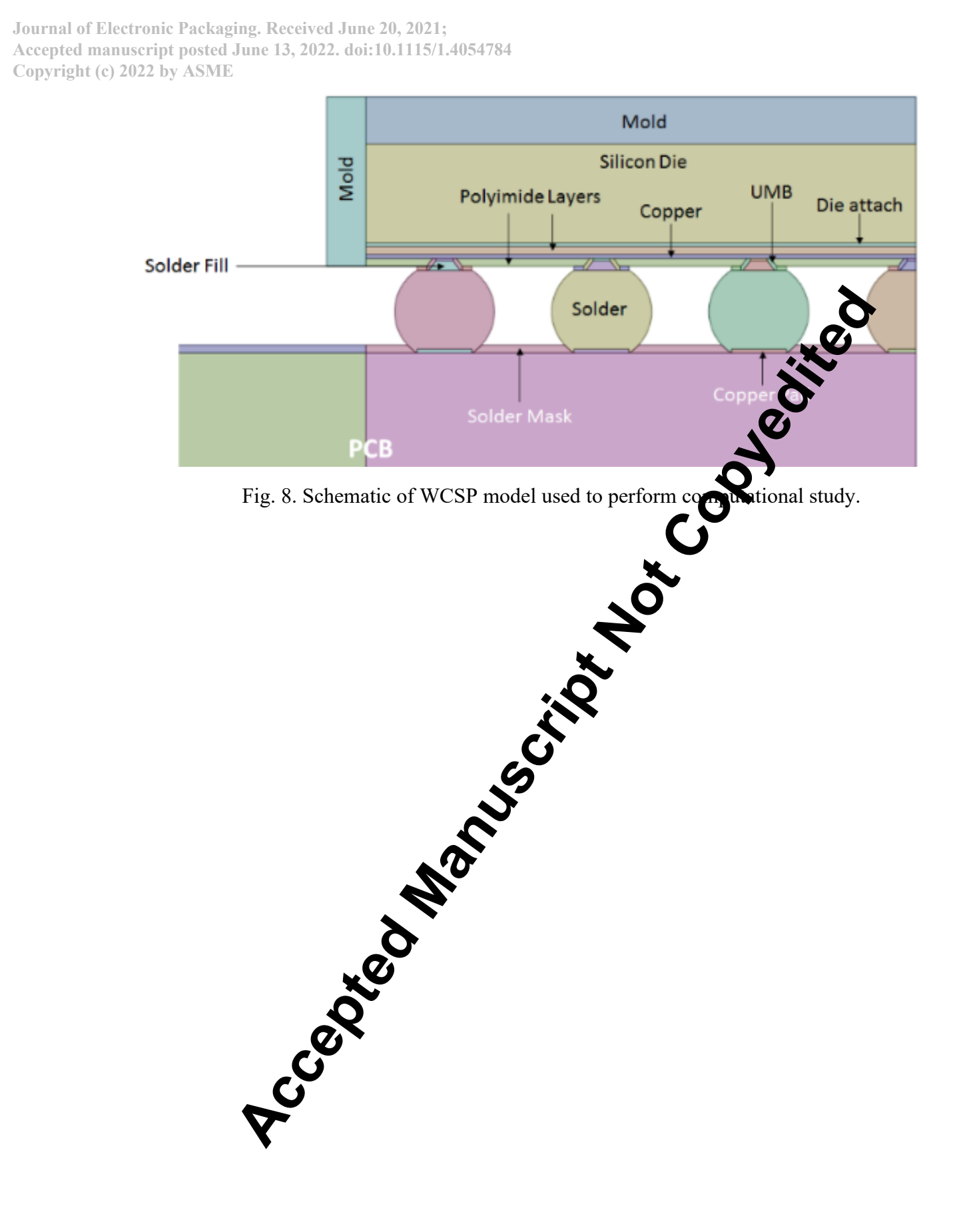
TABLE II PRONY SERIES TERMS FOR 155 °C AND 165 °C

155		°C	165 °C	
L	$\alpha_i^G$	$\tau_i^c$	$\alpha_i^{G}$	$\tau_i^{G}$
Inf	2.73E-01	N/A	2.73E-01	N/A
1	3.92E-02	4.03E-10	3.92E-02	2.49E-11
2	2.77E-02	1.97E-08	0.03	1.22E-09
3	3.48E-02	1.92E-06	3.48E-02	1.20E-07
4	6.40E-02	4.80E-05	2.72E-02	1.20E-07
5	1.05E-01	6.13E-04	6.40E-02	2.945-05
6	1.35E-01	5.40E-03	1.05E-01	3.8)E-05
7	1.35E-01	3.77E-02	1.35E-01	3.34E-04
8	1.01E-01	2.61E-01	1.35E-N	2.33E-03
9	5.80E-02	2.28	1.01E-01	1.61E-02
10	2.72E-02	43.79	0E-02	1.41E-01

#### III. COMP ATIONAL STUDY

#### A. Thermal Cycling

For the computational model, the PCP we extended to avoid edge effects. The chip used has a size of 2.8 x 2.8 mm with pitch is 0.4 mm and to 10.49 solder balls arranged in 7 x 7 array. Leveraging the symmetry of the models, quarter symmetry models were used [35]. Hex dominant and body sizing was used to mesh the critical component, solder balls one schematic of the WCSP model is given in Fig. 8 below. Detailed mesh model and boundary conditions used for the computational study are shown in Fig. 9. The material property of the different components used the computational study is given in Table III.





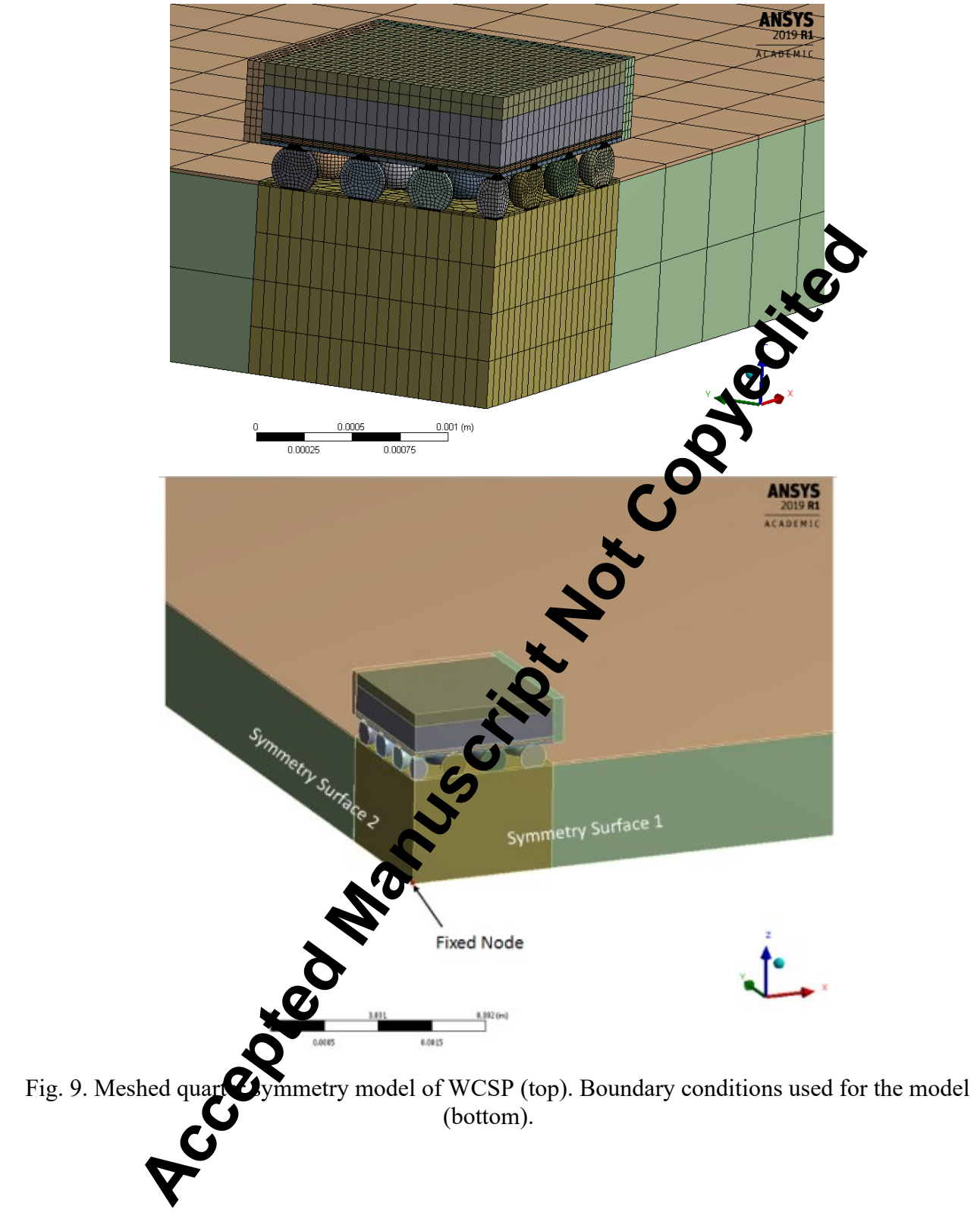


TABLE III
MECHANICAL PROPERTIES OF THE DIFFERENT COMPONENTS USED IN THE
COMPUTATIONAL STUDY [7] [36] [26] [37]

	E (GPa)	CTE (ppm/°C)	v
Cu	110	17	0.34
Die Attach	10	33	0.3
Mold	24	20	0.3
PCB	17	X, Y 13.2; Z: 50	0.20
Polyimide Layer	1.2	52	25
RDL	130	16.8	0.34
Die	131	3	0.28
Solder	55.3 @ -40 °C, 42 @ 25 °C, 33 @ 75 °C, 23 @ 125 °C	20,00	0.4
UBM	50	16	0.35
Solder Mask	4	00	0.4

VALUES FOR THE ANAND CONSTANTS USER A MODEL SOLDERS. PROPERTIES FOR SAC 387 GIVEN DELOW [18]

S. No	Constant	Unit	Value
1	s0 🖍	MPa	3.3
2	QA	1/K	9883
3	1	sec-1	1.57E+07
4	75	Dimensionless	1.06
5	m	Dimensionless	0.3686
0	h0	MPa	1077
	ŝ	MPa	3.15
8	n	Dimensionless	0.0352
<b>9</b>	a	Dimensionless	1.6832

Regardless of initial stress-free temperature, structure will readjust and reach a 'near-stress-free' at high-dwell temperature after few cycles. Stabilized values of strain or strain energy density per cycle are independent of the initial stress-free setting [26]. For the current study, the high-dwell temperature was selected as the zero thermal strain temperature. Condition G and H of JEDEC standard JESD22-A014D were used [38]. The corresponding temperature profiles are shown in Fig. 10. Fatigue cracks of solders occur at the package side near the interface of solder bulk/copper or UBM layer [26]. The damage parameters are extracted from 10 um layer of corner solder joint at the package side [26]. The inelastic energy density

accumulated per cycle is averaged over the volume of the thin disk (equation 13), and the resulting damage metrics is used to predict the number of cycles to failure [26] [39] [40].

$$\triangle W_{ave} = \frac{\sum_{i} W_{i} V_{i}}{\sum_{i} V_{i}} \tag{13}$$

The change in inelastic energy density after the third cycle was determined to be constant. This value was used because of computational costs and the solder joints have reached stability after third cycle [41]. An APDL code from [7] was used to compute the change in inelastic energy density. The model proposed by Schubert et. al. as shown in equation 14 below was used to find  $N_f$  [13].

$$N_f = \left(\frac{A}{\Delta W}\right)^k \tag{14}$$

The values of A and k were given as follows;  $A = 8.783 \times 10^6 \text{ MPa}$ , k = 0.4701 A

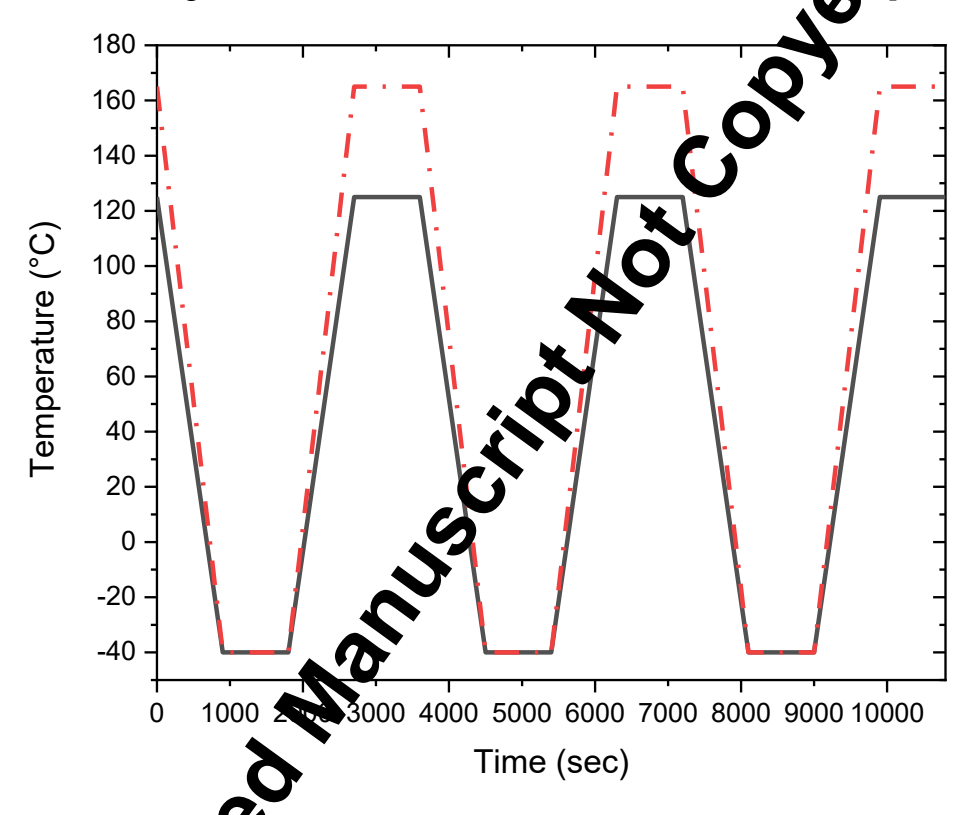


Fig. 10. Temperature cycling Mofiles used for the study: condition G (solid line) and H (dotted line) of EDEC standard JESD22-A014D are shown.

#### B. Drop Testing

WLP technology enables smaller, thinner, and faster electronic products, and has been widely used in portable electronic in facts. To understand the reliability of products under mechanical shock from customer usage or transportation, Joint Electron Device Engineering Council (JEDEC) has developed board designs and test standards that are used in assessing the reliability of handheld electronic products [42]. Due to the symmetry of the JEDEC board, quarter symmetry of it is used as shown in Fig. 11 [5].

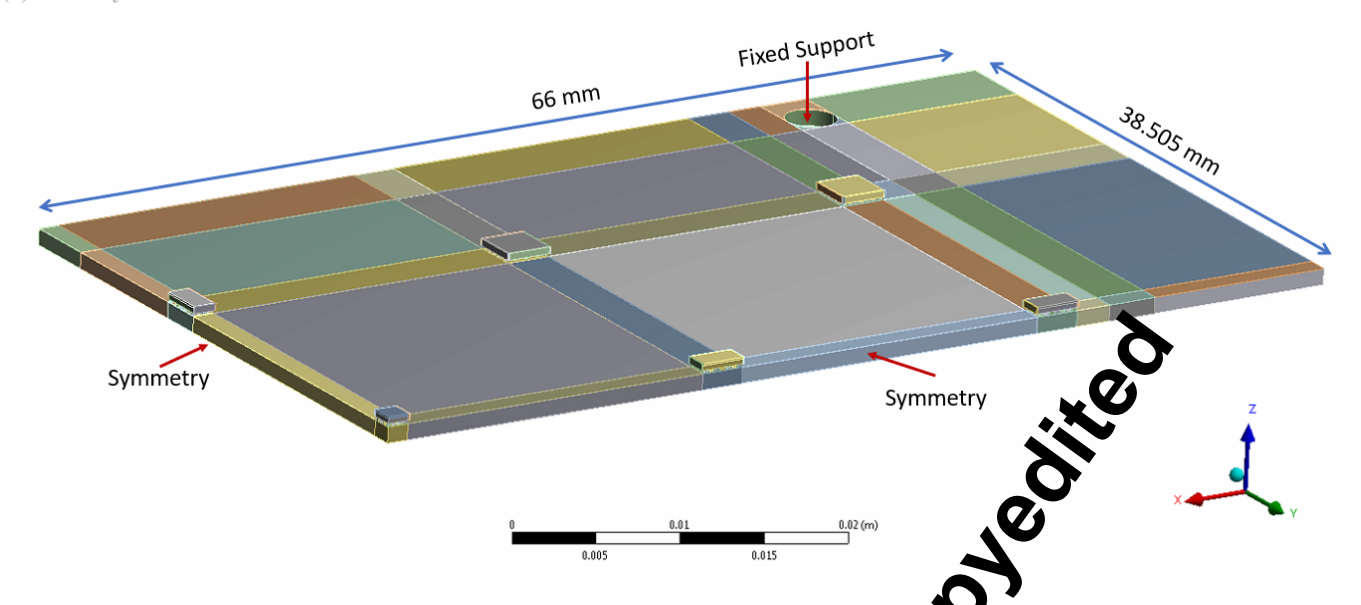


Fig. 11. Quarter symmetry of the JEDEC board used for the computational study.

For computational analysis of drop testing, different modeling teclniques have been developed. Dynamic vs. static analysis type, free-fall vs. input-G loads, explicit vs. implicit solvers, are some of the approaches that can be used for performing drop testing analysis [42]. For input-G method, components used in experimental testing (such as drop table, fixture, etc.) are not haveded in the simulation and their impact is captured by applying an impact impulse to the mounting hole [42]. Simulation results using explicit Input-G method have been shown to correlate well with experimental results [43]. On the other hand, Input-D method applies displacement at the loading points. Solutions for input-D and Input-G methods include rigid body movement. An alternative method, direct acceleration input (DAI) method removes the rigid body movement and is commonly used to perform drop dudy analysis. In the DAI method, acceleration impulse is applied as body force and the mounting holes as fixed during the dynamic response [42]. Equation 15 below shows the impulse conditions applied to in model.

$$\{M\}[\ddot{u}] + \{C\}[\dot{u}] + \{K\}[u] = \begin{cases} \{M\}1500g * \sin\frac{\pi t}{t_w}, \text{ where } t < t_w \} \\ 0, \text{ where } t \ge t_w \end{cases}$$

$$t_w = 0.5 \text{ m. Initial Conditions are } [x]|_{t=0} = 0, [\dot{x}]|_{t=0} = \sqrt{2gh}$$

$$\text{Boundary Conditions are } [x]|_{\text{at hole}} = 0$$

 $\{M\}$  is the mass matrix,  $\{u\}$  is the damping coefficient,  $\{K\}$  is the stiffness coefficient matrix. [u] is displacement vector,  $[\dot{u}]$  is elecity vector, and  $[\ddot{u}]$  is acceleration vector.

The JEDEC board was multiple components and hundreds of solder balls is a very big model and computationally extensive for FEA analysis. Sub-model technique needs to be applied to be obtain fast solutions while still obtaining accurate results. In the global model, the solder balls are simplified and represented as cubical blocks. For the sub-model, detailed structure components are added and simulated. The sub-model technique in ANSYS uses the solution of the global model and the cut boundary conditions for the local model. In this paper, the global model is used to make a comparative study in order to assess the impact of including viscoelastic properties on PCB under drop testing loading conditions.

#### IV. RESULTS

#### A. Thermal Cycling Results

The results for the computational study with the thermal cycling boundary conditions are given below. Table V shows the average inelastic energy density for the different cases investigated. Fig. 12 shows the comparison for the number of cycles to failure computed using equation 14 above.

TABLE V AVERAGE PLASTIC WORK (PA) FOR THE DIFFERENT THERMAL CYCLING ONDITIONS

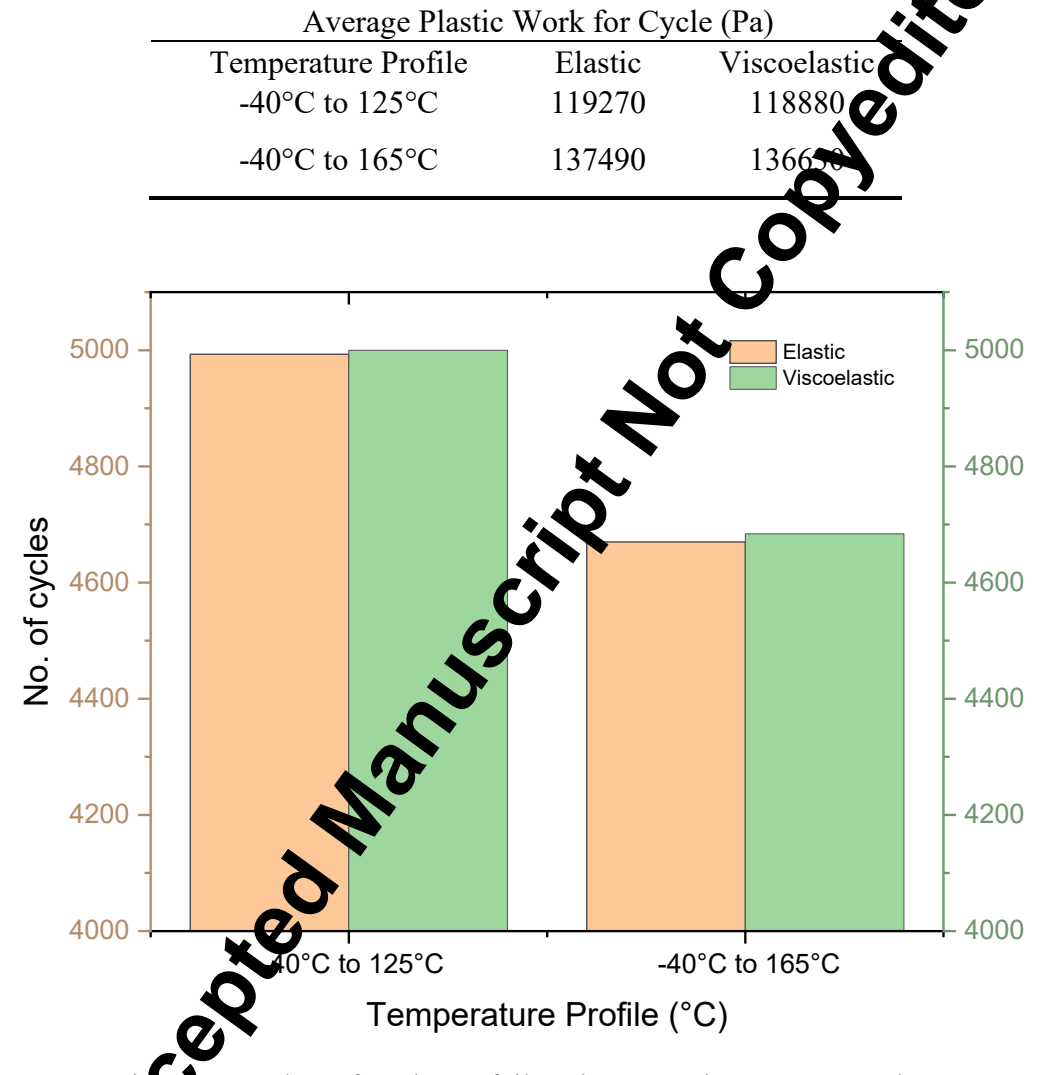


Fig. 12. Plot comparing the number of cycles to failure between the two cases where PCB were modeled elastic and viscoelastic.

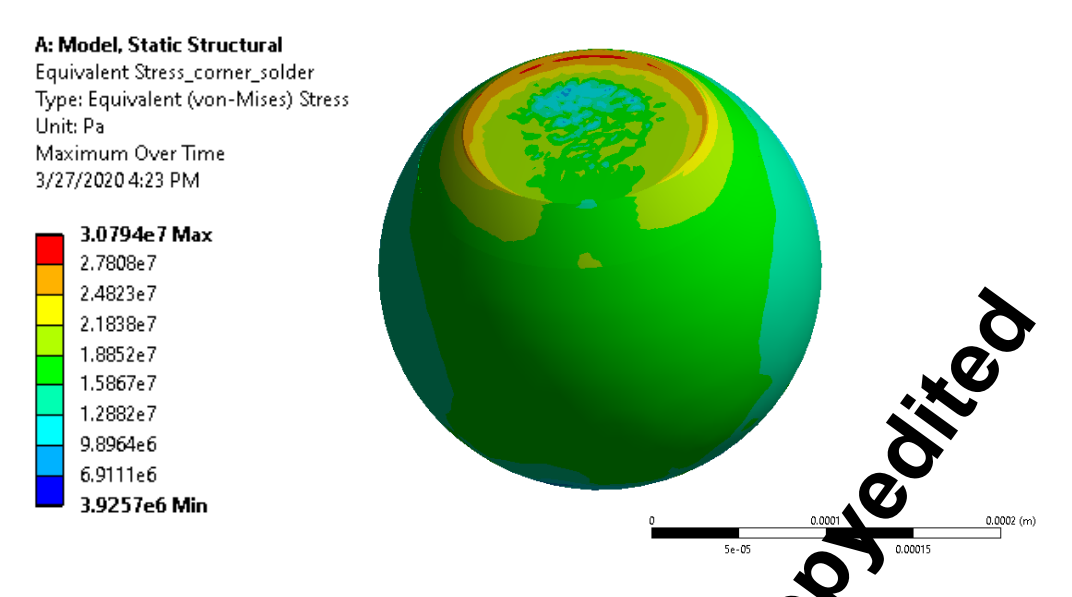


Fig. 13. Equivalent stress on corner solder for the elastic case for the maleycling for -40 °C to 165 °C.

#### B. Drop Testing Results

The results for the computational study with the drop testic an undary condition are given below. Fig. 14 shows the deformation of the quarter model for drop testing at 135°C where the PCB is modeled as viscoelastic material. Fig. 15 - Fig. 17 show the comparison between the two cases where the PCB was modeled as elastic and viscoelastic.

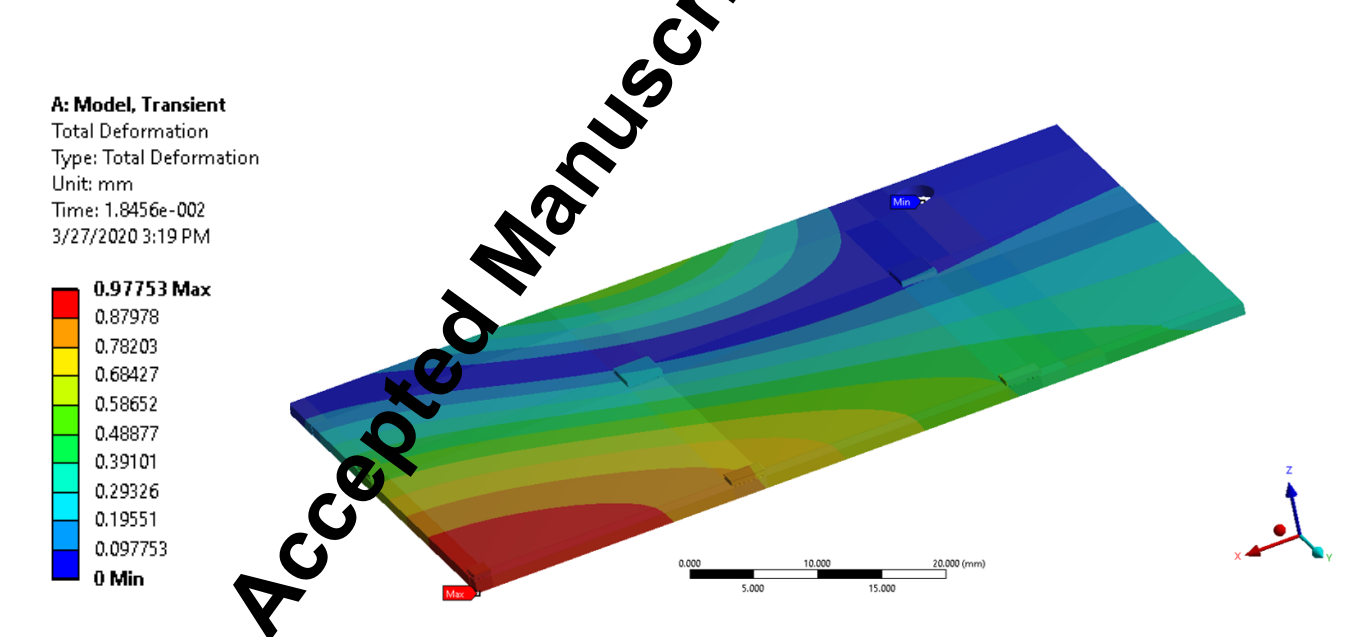


Fig. 14. Total deformation of the quarter symmetry model.

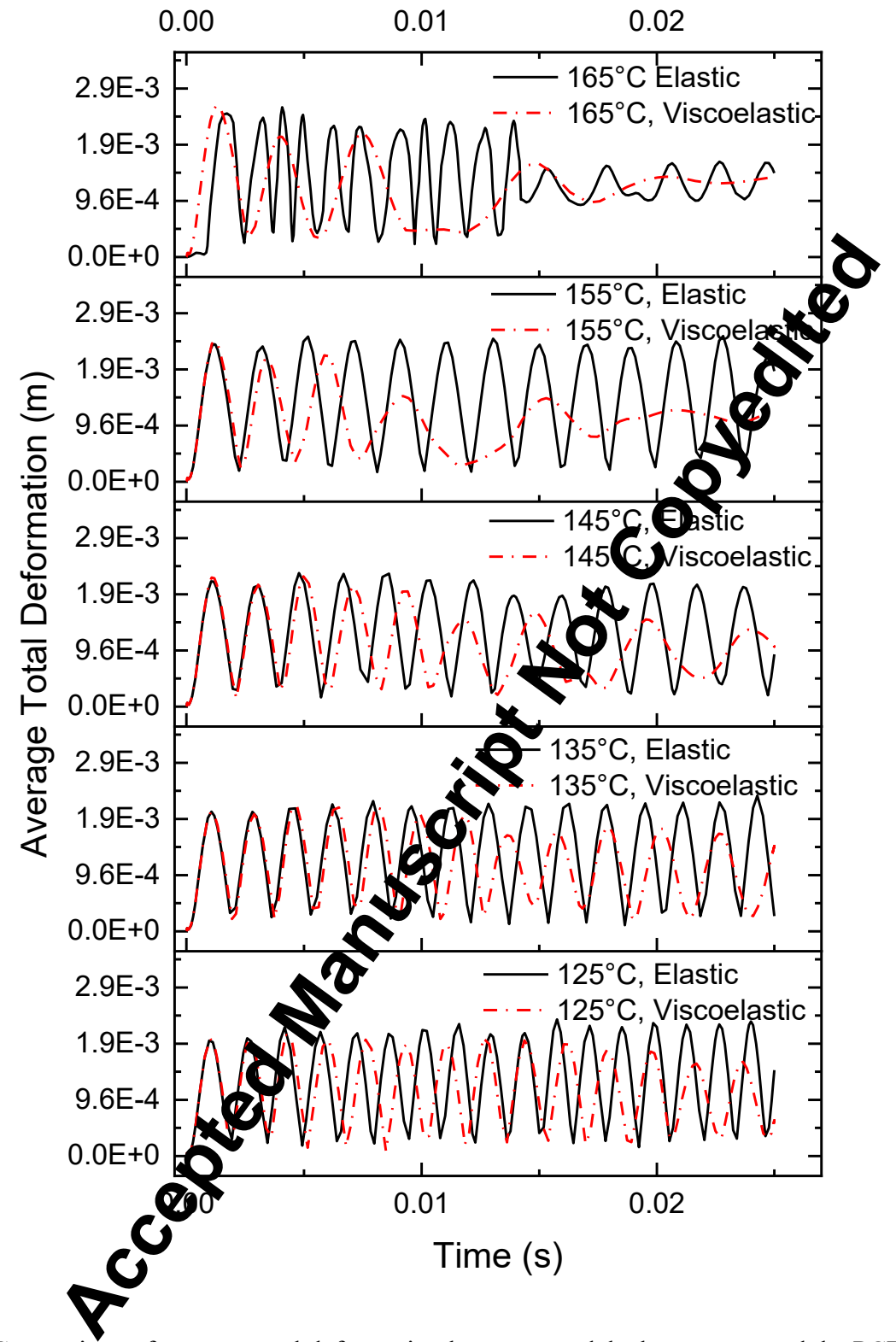


Fig. 15. Comparison of average total deformation between models that represented the PCB elastic and viscoelastic. Results shown for different temperatures.

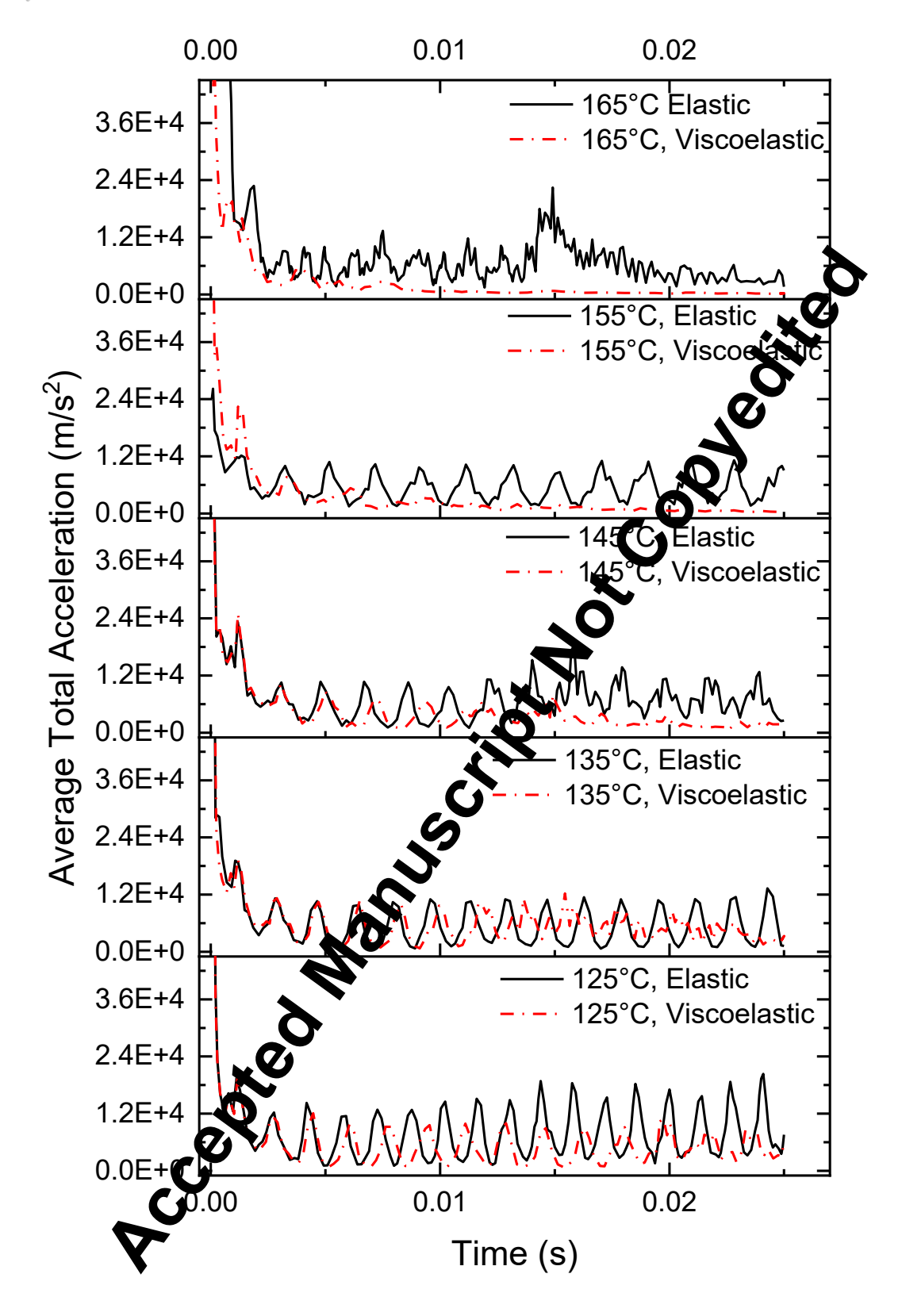


Fig. 16. Comparison of average total acceleration between models that represent the PCB as elastic and viscoelastic. Results shown for different temperatures.

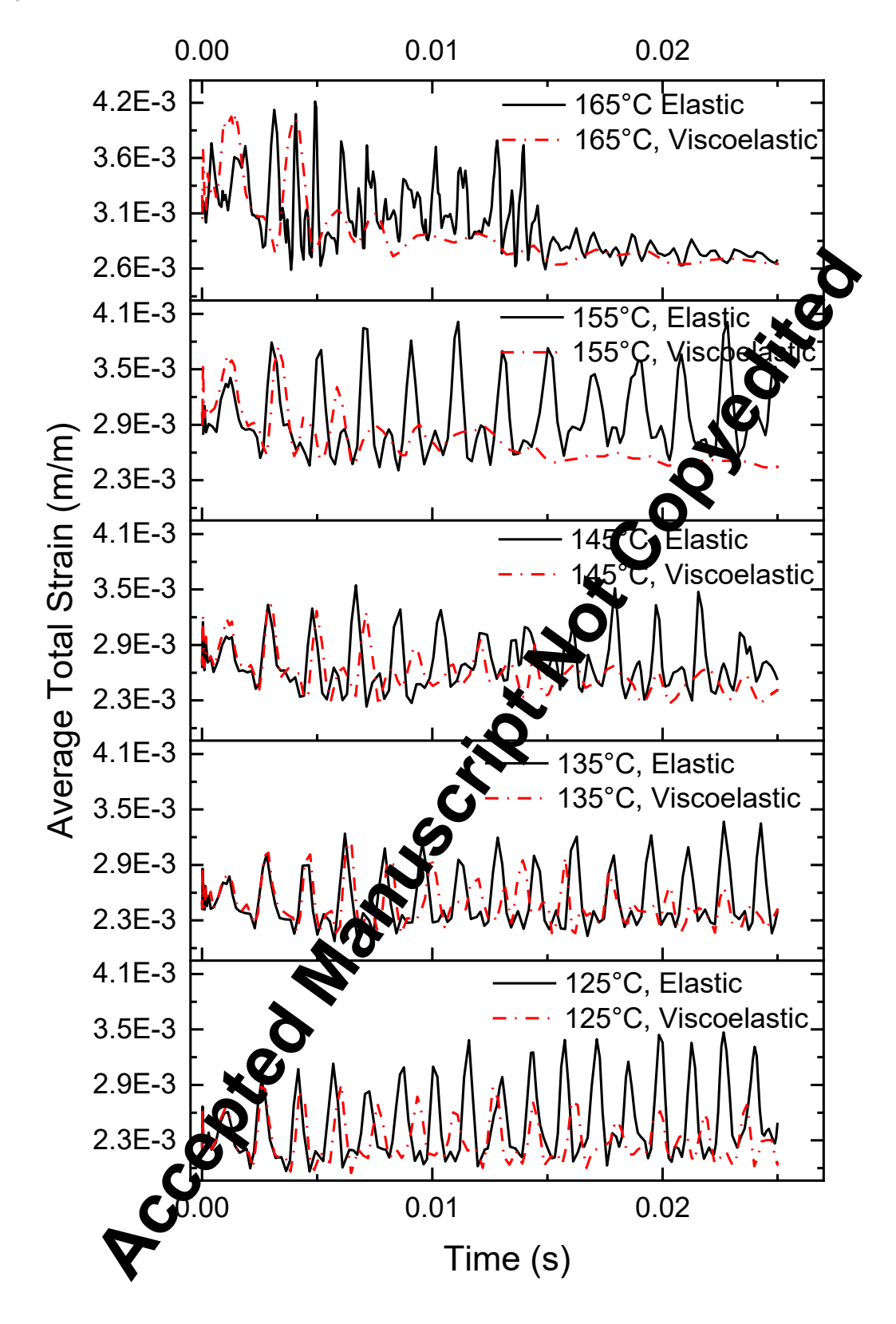


Fig. 17. Comparison of strain between models that represent the PCB elastic and viscoelastic. Results shown for different temperatures.

#### V. DISCUSSION and CONCLUSION

Previous studies that investigated the impact of viscoelastic influence of PCBs used different approaches to characterize the viscoelastic properties. Shrotriya et. al. [23] used creep data from DMA to develop a micromechanical model, while others [31] used time domain master curves to develop viscoelastic models. Rather than adding extra step to convert the frequency domain master curve to time domain, this paper characterizes the viscoelastic properties in term of Prony series terms directly from the frequency domain master cure. To determine the suitability of the PCB material for the time-temperature analysis using WLF method, 'wicket plot' was produced as shown in Fig. 6. The almost symmetrical curve of the wicket plot established the suitability of the DMA measurement of PCB for the WLF analysis and produce the master curve in the frequency domain. Fig. 4 shows temperature dependent storage and loss in colulus measurements for six different frequencies. Using the WLF shift function, the frequency domain in other curve shown in Fig. 5 was obtained. The corresponding Prony series terms were obtained from non-linear fit (shown in Table II) and included in the subsequent finite element analysis. Fig. 7 shows a comparison between the computed and experimentally measured frequency dependent storage, and complex nodures values. The difference between the computed and experimentally measured values was found to be an average less than 1%.

The thermal cycling results on the WLP package are shown in section 4.1. Condition G and H of JEDEC JESD22-A014D standard were used to apply the thermal boundary conditions. Simulation was run for three cycles, and the difference in average inelastic energy density between the third and second cycles was computed and tabulated in Table V. Equation 14 was then used to compute the number of cycles to failure. Fig. 12 shows the computed cycle to failure for the difference cases investigated. It is shown that for both condition G and H thermal cycling conditions, the difference between the models with the PCB modeled elastic and viscoelastic is negligible. For failures under thermal cycling, the CTE mismatch between PCB and die is the main contributing factor. As a result, the necessity been reported in literature [31] [32]. The previous studies converted the frequency domain master drives to time domain before obtaining the Prony series terms. In this paper, it has been shown that frequency domain master curve results from dynamic mechanical analysis can be used to characterize the viscoelastic behavior of PCBs and perform computational analysis.

In section 4.2, results for drop testing simulations are shown. The computational results for strain, deformation, and acceleration are shown Fig. 15 - Fig. 17. The comparisons were done for drops at different temperatures. The glass transition temperature was measured to be 126.5 °C. Temperatures closer to and significantly higher than the Tg were closen for the comparison. For comparison at 165 °C, the deformation, strain, and acceleration are over dedicted for the case where the viscoelastic property of PCBs is not included. Previous work done by Liu et. al. has shown that the increase in viscosity of the PCB will dampen the responses under drop testing conditions [24]. Moreover, Kraemer et. al. found that the FEM simulation of drop test overestimated the stress and strain at the copper trace of PCB which did not match experimental results [44]. Other work has also shown that the time-temperature dependent behavior of PCB substrates is important to understand esidual stresses and dimensional changes in the PCBs during processing such as relamination and sold ring processes [23]. This shows that for applications where temperatures go above the glass transition temperature and a drop testing boundary condition is used, it is important to include the viscoelastic property of PCBs in order to accurately capture the system behavior.

In summary, for computational studies with both Condition G and H of JESD22-A014D standard, it is shown that the inclusion of viscoelastic properties did not impact the computational results. For computational studies with drop testing boundary conditions, it is shown that for temperatures above the

glass transition temperature, the inclusion of viscoelastic properties has significant impact on the board level analysis of deformation, strain, and acceleration. However, for temperatures below glass transition temperature, the inclusion of the viscoelastic properties is not necessary which will save the computational cost during the design and modeling of the PCBs. In this study, nonlinear fitting tools were successfully used on frequency domain master curve results from dynamic mechanical analysis to characterize the viscoelastic behavior of PCBs and computationally study the impact of PCB modeling. This approach has a great advantage as it does not require the conversion of results to time domain. However, one limitation of this approach is in characterizing soft materials such as thermal interface materials (TIMs) and die attach materials as these materials have very low glass transition temperatures and pose a challenge in obtaining as stic proper data to generate master curves from DMA measurements. A future work from this study buld be addressing these challenges and extending the use of this technique to study the viscoelastic properties of soft materials such as TIMs and die attach materials.

## **NOMENCLATURE**

```
Stiffness of j<sup>th</sup>
  k_i
                         Damping of jth
  \tau_i
                         Applied stress
  σ
 G(t)
             Shear modulus as a function of time
                    Shear modulus at t = 0
  G_0
 \alpha_{\infty}^{G}
             Long term Prony coefficient (shear)
                    relative Moduli (G<sub>i</sub>/G<sub>0</sub>)
                        relaxation times
                       Relaxation modes
  n_G
                               Time
   t
  G^*
                   Complex shear modulus
  G_{\infty}
                   Long term shear modulus
                      ith Prony series term
                    Storage shear modulu
  G'
  G^{\prime\prime}
                      Loss shear modu
  E^*
                       Complex modulu
  E'
                        Storage mod
  E^{\prime\prime}
Tan \delta
  a_T
  T
  T_r
                    Reference temperature
  T_g
                 Glass ransition temperature
                        fficient of shift factor
  C_1
               Second coefficient of shift factor
  C_2
                            Frequency
  ω
                            \tau = 1/t
   τ
                 Initial value of deformation
  S_0
                           resistance
```

Q/R	Activation energy/Boltzmann's
	constant
A	Pre-exponential factor
ξ	Stress multiplier
m	Strain rate sensitivity of stress
h0	Hardening/softening constant
ŝ	Coefficient for saturation value of
	deformation resistance
n	Strain rate sensitivity of the
	saturation value
a	Strain rate sensitivity of the
	hardening/softening

#### **REFERENCES**

- [1] L.-T. Yeh and R. C. Chu, Thermal Management of Microelectronic Equipment, New York: ASME Press, 2002.
- [2] W. Hilbert and F. Kube, ""Effects on Electronic Equipment Reliability of Temperature Cycling in Equipment," Report No. EC-69-400 (Final Report)," Grumman Aircraft Corp., Feb page, NY, 1969.
- [3] W. Engelmaier, "Solder Joints in Electronics: Design for Reliability," Keynote Address in Design and Reliability of Solder and Solder Interconnectons, 1997, pp. 9-19.
- [4] "Guidelines for Accelerated Reliability Testing of Surface Sound Solder Attachments," IPC Guidelines IPC-SM-785. The Institute of Interconnecting and Packaging Electronic Circuits., Lincolnwood, IL, November 1992.
- [5] JESD22-B111, "Board Level Drop Test Method of mponents for Handheld Electronic Products," JEDEC SOLID STATE TECHNOLOGY ASSOCIATION, 2003.
- [6] M. M. Hossain, S. Jagarkal, D. Agonafer, J. Juliu and S. Reh, "Design Optimization and Reliability of PWB Level Electronic Package," *Journal of Electronic Packaging*, vol. 129, no. 1, pp. 9-18, 2007.
- [7] B. A. Zahn, "Finite Element Based Solder Joint Fatigue Life Predictions for a Same Die Stacked Chip Scale Ball Grid Array Package," 27th Annua LEEE/SEMI International Electronics Manufacturing Technology Symposium. IEEE, 2002.
- [8] S. Yamada, "A Fracture Methanics Approach to Soldered Joint Cracking," *IEEE CHMT*, vol. 12, no. 1, pp. 99-104, 1989.
- [9] W. Engelmaier, "Functional Cycling and Surface Mounting Attachment Reliability," *ISHM Technical Monograph Series 6894-00*2, 87-114, 1984.
- [10] A. Syed, "Creep Crack Growth Prediction of Solder Joints During Temperature Cycling An Engineering Approach," *Transactions of the ASME*, vol. 117, pp. 116-122, 1995.
- [11] R. Darveaux, K. Baneerji, A. Mawer and G. Dody, "Reliability of Plastic Ball Grid Array Assembly," in *Ball Grid Array Technology*, New York, McGraw-Hill Inc., 1995, pp. 379-442.

- [12] S. Liu and Y. Liu, Modeling and Simulation for Microelectronic Packaging Assembly: Manufacturing, Reliability and Testing, Singapore: Chemical Industry Press, 2011.
- [13] A. Schubert, R. Dudek, E. Auerswald, A. Golhardt, B. Michel and H. Reichi, "Fatigue Life Models for SnAgCu and SnPb Solder Joints Evaluated by Experiments and Simulation," in *53rd Electronic Components and Technology Conference*, *2003. Proceedings.*, New Orleans, Louisiana, 2003.
- [14] L. Anand, "Constitutive Equations for the Rate-Dependent Deformation of Metals at Elevated Temperatures," *Journal of Engineering Materials and Technology*, vol. 104, no. 1, pp. 12-17, 1982.
- [15] S. Brown, K. Kim and L. Anand, "An Internal Variable Constitutive Model for Hot Working Metals," International Journal of Plasticity, vol. 5, no. 2, pp. 95-130, 1989.
- [16] M. Motalab, Z. Cai, J. C. Suhling and P. Lall, "Determination of Anand constants for AC Solders using Stress-Strain or Creep Data," in 13th IEEE ITHERM Conference, San Diego, CA, 2012.
- [17] T. C. Lui, "Lifetime Prediction of Viscoplastic Lead-free Solder," in *Internation Workshop on Integrated Power Packaging*, TU Delft, Netherlands, 2017.
- [18] D. Bhate, D. Chan, G. Subbarayan, T. Chiu, V. Gupta and D. Edwards, "Constitutive behavior of Sn3.8Ag0.7Cu and Sn1.0Ag0.5Cu alloys at creep and low strain rate regimes," *IFFS Hansactions on Components and Packaging Technologies*, vol. 31, no. 3, pp. 622-633, 2008.
- [19] M. Mottahedi, A. Dadalau, A. Hafla and A. Verl, "Numerical analysis of relaxation test based on Prony series material model," *Integrated Systems, Design and Technology*, pp. 79-91, 2010.
- [20] S. W. Park and Y. R. Kim, "Fitting Prony-series Viscoel stic Models with Power-law Presmoothing," *Journal of materials in Civil Engineering*, vol. 13, no. 1, pp. 26 32, 2001.
- [21] M. Fernanda, P. Costa and C. Ribeiro, "Parametr sestimation of viscoelastic materials: a test case with different optimization strategies," *AIP Conference Proceedings*, vol. 1389, no. 1, pp. 771-774, 2011.
- [22] H. H.-T. Corporation, "Principle of Dynam Mechanical Analysis (DMA). https://www.hitachi-hightech.com/global/products/scie..." ech/ana/thermal/descriptions/dma.html," 2018.
- [23] P. Shrotriya and N. R. Sottos, "Cr en and Relaxation Behavior of Woven Glass/Epoxy Substrates for Multilayer Circuit Board Applications," *Proviner Composites*, vol. 19, no. 5, pp. 567-578, 1998.
- [24] F. Liu, G. Meng and M. Zhr 7, Viscoelastic Influence on Dynamic Properties of PCB Under Drop Impact," Journal of Electronic Parallel, vol. 129, pp. 266-272, 2007.
- [25] C. E. Miller, V. Ganchi and T. MacDonald, "Improving Reliability of Electronic Packages," in *ANSYS*, 20 April 2017.
- [26] X. Fan, B. Varia and Q. Han, "Design and Optimization of thermo-mechanical reliability in wafer level packaging," *Microelectronics Reliability*, vol. 50, no. 4, pp. 536-546, 2010.
- [27] TA Instruments., *Measurement of the Glass Transition Temperature Using Dynamic Mechanical Analysis.*, Thermal Analysis and Rheology. TA Instruments..

- [28] Hitachi High-Tech Science Corporation, *Instruction Manual: DMA Master Curve Analysis. Thermal Analysis Software TA7000.*, 0503-YB1-003E Ver.1.3., 2016.
- [29] R. Li, "Time-temperature superposition method for glass transition temperature of plastic materials," *Materials Science and Engineering: A,* vol. 278, no. 1-2, pp. 36-45, 2000.
- [30] R. Lakes, Viscoelastic Solids, Boca Raton, FL.: CRC Press LLC, 1998.
- [31] A. Anaskure, "Effect of Viscoelastic Modeling of PCB on the Board Level Reliability of Wafe Ship Scale Package(WCSP) In Comparison to Orthotropic Linear Elastic Modeling," Dissertation., 2012
- [32] A. Misrak, A. Anaskure, A. Sakib, U. Rahangdale, A. Lohia and D. Agonafer, "Compark in the effect of elastic and viscoelastic modeling of PCBs on the assessment of board level reliability.," in (0.3) 16th IEEE Intersociety Conference on Thermal and Thermomechanical Phenomena in Electronic System (1) therm). IEEE., Orlando, FL., May 2017.
- [33] K. Reddy and N. S. Reddy, "Comparative Study of Viscoelastic Modeling and hear Modeling for Wafer Level Chip Scale Package Under Drop Impact," Dissertation, 2017.
- [34] E. Barbero, M. Julius and Z. Yao, "Time and Frequency Viscoelastic Behavior of Commercial Polymers," Calabria, Italy. CCCC., 2003.
- [35] A. Mahnood, T. Barua, N. Sakib and D. Agonafer, "Impact of Cap Layer Orientation on the Drop Reliability of WCSP Boards," in *IEEE 66th Electronic Components and Technology Conference (ECTC)*, Las Vegas, 2016.
- [36] P. Rajmane, H. Khan, A. Doiphode, U. Rahangdale, D. You after, A. Lohia, S. Kummerl and L. Nguyen, "Failure mechanisms of boards in a thin wafer level chip scale nackage," in 16th IEEE Intersociety Conference on Thermal and Thermomechanical Phenomena in Electionic Systems (ITherm). IEEE, Orlando, FL, 2017.
- [37] R. Darveaux, "Thermal cycle fatigue life prediction for flip chip solder joints," 2014 IEEE 64th Electronic Components and Technology Conference (ECC), 2014.
- [38] JEDEC STANDARD, Temperature Cyclica, 2022-A104D, JEDEC Solid State Technology Association, March 2009.
- [39] D. R., "Solder joint fatigue life m Ge," in In: Proceedings of the TMS annual meeting, p. 213 8, 1997.
- [40] S. A., "Predicting solder joint enability for thermal, power, & bend cycle within 25% accuracy," *51st ECTC*, pp. 255-63, 2001.
- [41] J.-H. Zhao, V. Gupta, Actionia and D. Edwards, "Reliability Modeling of Lead-Free Solder Joints in Wafer-Level Chip Scale Packager," Journal of Electronic Packaging, vol. 132, no. 1, pp. 011005-1, 2010.
- [42] H. S. Dhiman, X. Zin and T. Zhou, "JEDEC Board Drop Test Simulation for Wafer Level Packages (WLPs)," in *Electronic Components and Technology Conference*, San Diego, CA, May 26 2009.
- [43] J.-e. Luan and T. Y. Tee, "Novel Board Level Drop Test Simulation using Implicit Transient Analysis with Input-G Method," in *Electronics Packaging Technology Conference*, Singapore, Singapore, 2004.

[44] F. Kraemer, S. Wiese, S. Rzepka, W. Faust and J. Lienig, "A detailed investigation of the failure formation of copper trace cracks during drop tests," in *3rd Electronics System Integration Technology Conference ESTC*, Berlin, 2010.

Accepted Manuscript. Not. Convenited